JACS
JOURNAL OF THE AMERICAN CHEMICAL SOCIETY

ARTICLE

pubs.acs.org/JACS

# Dynamics of Carbene Cycloadditions

Lai Xu,[†] Charles E. Doubleday,[*,‡] and K. N. Houk[*,†]

[†]Department of Chemistry and Biochemistry, University of California, Los Angeles, California 90095-1569, United States

[‡]Department of Chemistry, Columbia University, New York, New York 10027, United States

Supporting Information

**ABSTRACT:** Quasiclassical trajectory calculations using quantum mechanical energies and forces generated by the Venus and Gaussian programs provide for the first time a detailed dynamical picture of singlet carbene, $CCl_2$ and $CF_2$, cycloadditions to alkenes on the B3LYP/6-31G* surface. For $CF_2$, B3LYP/6-31G* with exact exchange reduced to 12% HF was also employed to better mimic the high accuracy surface. The range of geometries sampled in reactive trajectories and the timing of bond formation were explored. All trajectories follow the nonlinear approach proposed by Moore and Hoffmann. The reaction of $CCl_2$ with ethylene is a dynamically concerted reaction, with an average time gap between formation of the two bonds of 50 fs. The reaction of $CF_2$ with ethylene is dynamically complex with biexponential decay of the diradical species formed from the first bond formation. A general quantitative dynamical classification of cycloaddition mechanisms is proposed, based on the timing of bond formation.

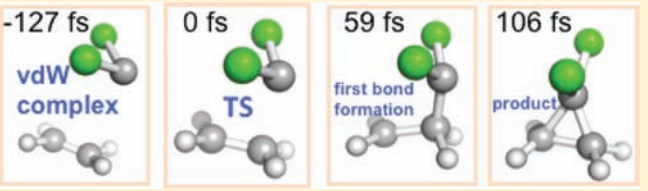


## INTRODUCTION

Carbene cycloadditions to alkenes have been known since the 1950s. Shortly after Hine discovered the intermediacy of dichlorocarbene in the hydrolysis of chloroform,[1] Doering and Hoffmann[2] found that $CCl_2$ could be captured by alkenes to yield cyclopropanes. These reports initiated over a half century of sophisticated research on the chemistry of carbenes leading to current views of mechanism. Here, we provide a time-resolved view of the mechanism of cycloadditions of singlet carbenes to alkenes.

Skell and Garner[3] postulated simultaneous bonding of the carbene carbon to both alkene carbons, leading to "three-center-type" interactions. In 1963, Moore proposed that the bonding in the transition state stems from overlap of the vacant p-orbital of the carbene with the $\pi$ orbital of the alkene.[4] In 1968, Hoffmann showed that the $C_{2v}$ symmetrical cyclic four-electron transition state is orbital symmetry forbidden,[5] one of the landmark predictions of orbital symmetry theory. A nonleast-motion transition state was proposed instead. Many calculations confirmed this picture of the transition state.[6] A connection between theory and experiment came from the good agreement between high-precision experimental kinetic isotope effects for the addition of singlet $CCl_2$ to pent-1-ene and the corresponding quantities computed with density functional theory for the transition state of a nonlinear path.[7]

Despite developments in molecular dynamics calculations involving quasiclassical trajectory simulations,[8] there are no reports of computed dynamics trajectories for these fundamental reactions. In 1973, Wang and Karplus reported direct dynamics CNDO trajectory calculations on the reaction of singlet $CH_2$ with $H_2$ in a *J. Am. Chem. Soc.* communication entitled "Dynamics of Organic Reactions".[9] This is the only report of trajectories computed for carbene additions or cycloadditions. They demonstrated that the detailed mechanism of such a bimolecular reaction is considerably more complex than is suggested by an analysis of the minimum energy reaction path.

We now provide for the first time a detailed dynamical picture of carbene cycloadditions of two typical singlet carbenes, $CCl_2$ and $CF_2$, to ethylene by quasiclassical trajectory calculations.[8] The nonleast motion approach is always strongly favored and leads to substantial asynchronicity in bond formation. The timing of bond formation has been determined and compared to these quantitities computed earlier for 1,3-dipolar cycloadditions and Diels–Alder cycloadditions.[10] A dynamical classification of cycloaddition mechanisms is proposed.

## COMPUTATIONAL METHODOLOGY

Table 1 shows the energies of stationary points on the potential energy surfaces for additions of $CCl_2$ and $CF_2$ to ethylene at different levels of theory. For both reactions, application of UB3LYP/6-31G* (spin-unrestricted B3LYP) with and without the DFT-D3 dispersion correction[11] gives qualitatively similar results. In particular, use of DFT-D3 gives a lower energy initial carbene–olefin complex. The $CCl_2$ addition has a very low barrier and no intermediate diradical. For the $CF_2$ reaction, two additional methods are included: the recent MRMP2 results of Nagase and co-workers[6i] and mUB3LYP, an ad hoc modification of UB3LYP described below. UB3LYP predicts a shallow diradical minimum for $CF_2$ + ethylene, both with and without DFT-D3. Neither MRMP2 nor mUB3LYP predicts a diradical minimum.

Figure 1 shows intrinsic reaction coordinate (IRC) reaction paths for $CCl_2$ and $CF_2$ cycloadditions. There is good agreement in the addition

**Received:** August 2, 2011
**Published:** September 30, 2011

  

**Table 1. Relative Energies $\Delta E$ without ZPE Corrections and Relative Enthalpies $\Delta H$ (kcal/mol, B3LYP/6-31G* Unless Noted) for the Reaction of $CCl_2$ and $CF_2$ with Ethylene**

| | $CCl_2$ + ethylene | | | |
|---|---|---|---|---|
| | reactants | van der Waals complex | TS | product |
| $\Delta E$ | 0.0 | −1.1 | 0.5 | −67.8 |
| $\Delta E$ (B3LYP/6-31G* + DFTD3//B3LYP/6-31G*) | 0.0 | −3.4 | −3.3 | −71.0 |
| $\Delta H$ | 0.0 | 0.1 | 1.4 | −64.3 |

| | $CF_2$ + ethylene | | | | | |
|---|---|---|---|---|---|---|
| | reactants | van der Waals complex | addition TS | diradical | closure TS | product |
| $\Delta E$ | 0.0 | −1.4 | 7.5 | −2.5 | −1.6 | −52.2 |
| $\Delta E$ (B3LYP/6-31G* + DFTD3//B3LYP/6-31G*) | 0.0 | −2.7 | 5.4 | −4.6 | −3.9 | −54.1 |
| $\Delta E$ (mUB3LYP/6-31G*//mUB3LYP/6-31G*) | 0.0 | −1.6 | 4.9 | NA | NA | −53.5 |
| $\Delta E$[6i] (MRMP 2(4,4)/6-311+G(d,p)//CASSCF(4,4)/6-31G(d,p) | 0.0 | *a* | 13.3 | −2.5 | −4.7 | −53.9 |
| $\Delta H$ | 0.0 | −0.7 | 8.1 | −1.0 | −0.6 | −48.9 |

[a] Not reported in ref 6i.

barriers between DFT (UB3LYP and mUB3LYP) and multireference perturbation theory. In both reactions, and at all levels of theory, the IRCs go through an intermediate flat region in which only one C−C bond has been formed. For $CF_2$ + ethylene, UB3LYP and MRMP2-(10,10) predict the same addition barrier with respect to the $CF_2$/ethylene complex. After the barrier is crossed, however, MRMP2 has a nearly flat shoulder, while UB3LYP predicts a minimum with a 1 kcal/mol barrier to cyclization. Although the UB3LYP barrier is shallow, its presence may affect the dynamics by lengthening the lifetime of the intermediate. To test the effect on the dynamics of removing the barrier, we sought to modify UB3LYP to remove the barrier, then run trajectories on the resulting surface. Because Hartree−Fock theory favors double occupancy of orbitals that leads to spurious minima in biradicals, we reduced the fraction of Hartree−Fock exchange in UB3-LYP from 20% to 12%, with a compensatory adjustment in the contribution of local exchange to 88%, leaving unchanged the contributions of nonlocal exchange and local and nonlocal correlation. The modified functional is called mUB3LYP.[12] The mUB3LYP IRC for $CF_2$ + ethylene is shown in green in Figure 1. The shallow minimum has been eliminated, but in addition about one-half the flat region has also been removed. We shall return to this feature when we discuss the dynamics.

The reactions of $CCl_2$ and of $CF_2$ with ethylene were explored with 512 quasiclassical trajectories using UB3LYP/6-31G*. The reaction of $CF_2$ with ethylene was also explored with 333 quasiclassical trajectories using mUB3LYP/6-31G*. These were computed with Doubleday's customized version of the Venus dynamics program.[13] In the option used here, Venus is used to select initial coordinates and momenta by TS normal mode sampling,[14] and the trajectories are integrated by Gaussian 09[15] using the Born−Oppenheimer molecular dynamics model with the option of reading initial Cartesian velocities from the input stream. The sampling procedure generates a set of structures whose coordinates and momenta approximate a quantum mechanical Boltzmann distribution of vibrational levels on the TS dividing surface at 298 K. All of the trajectories begin in this transition state region and are run in both forward and reverse directions from the initially selected point. Trajectories are accepted if one segment (forward or backward) forms the adduct and the other segment forms reactants. For 90% of dichloro trajectories and 97% of difluoro (UB3LYP and mUB3LYP), energy is conserved to within 0.1 kcal/mol or less.

Sampling of initial conditions was carried out at the UB3LYP/6-31G* saddle points for the reaction of $CCl_2$ and $CF_2$ with ethylene, and also with mUB3LYP/6-31G* saddle point for $CF_2$ + ethylene in Figure 1. These transition structures are somewhat earlier and looser than the canonical variational TSs.[16,17] The main effect of sampling at the conventional transition state is that a larger fraction of unreactive trajectories are sampled than would be the case if the variational TSs were sampled. However, the internal dynamics of the adducts are not expected to be sensitive to this source of sampling error. Unproductive and recrossing trajectories constitute 12% of the trajectories for $CCl_2$ + ethylene, and 10% and 9%, respectively, for UB3LYP/6-31G* and mUB3LYP/6-31G* trajectories for $CF_2$ + ethylene. These may result in large part from starting at geometries on the reactant side of the VTS.

## RESULTS AND DISCUSSION

**Overlay of Sampled Initial Geometries.** Figure 2 shows the overlay of sampled starting geometries in (a) each of the 453 reactive trajectories for $CCl_2$ + ethylene, (b) 466 reactive trajectories on the UB3LYP/6-31G* surface, and (c) 298 reactive trajectories on the mUB3LYP/6-31G* surface for $CF_2$ + ethylene. The initial structures for the reaction of $CCl_2$ with ethylene are scattered, which is consistent with the very low barrier and early transition state. The overlay of structures for the reaction of $CF_2$ with ethylene is tighter than that for $CCl_2$ due to the more advanced transition state.

**Snapshots of Representative Trajectories.** Figure 3 shows snapshots of representative trajectories for the reactions of $CCl_2$ and $CF_2$ with ethylene. For the $CCl_2$ + ethylene trajectory in Figure 3a, the time gap between formation of the two bonds of cyclopropane (defined as a C−C distance <3.0 bohr or 1.59 Å)[18] is 47 fs.

Figure 3b and c shows snapshots of a representative trajectory for $CF_2$ + ethylene on the UB3LYP/6-31G* and mUB3LYP/6-31G* surface, respectively. In Figure 3b, the time gap between

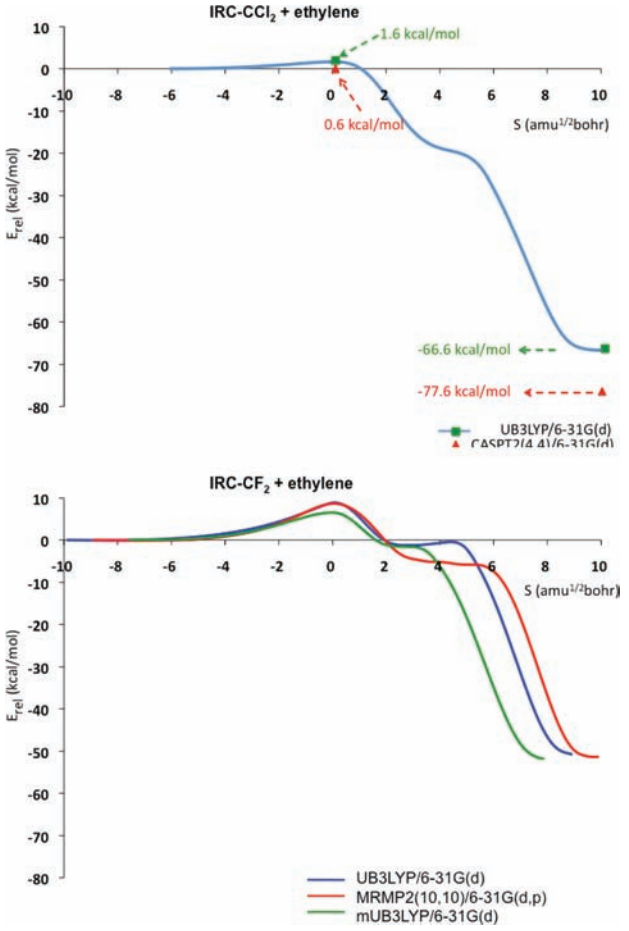


**Figure 1.** IRC path of the reaction of $CCl_2$ and $CF_2$ with ethylene. The data for the reaction of $CF_2$ with ethylene are taken from Nagase and co-workers.[6i] In each case, the zero of energy is the $CX_2$/ethylene complex.

bond formations is 245 fs; in Figure 3c, it is 118 fs. Trajectory animations have been placed on the Website http://www.chem.ucla.edu/~lxu01pku/carbene_dynamics.

The trajectories in Figure 3 display three features shared in common by all trajectories for $CCl_2$ and $CF_2$ additions to ethylene: that (1) formation of the two bonds is always sequential, never synchronous, (2) cyclization step occurs only when the pyramidal $CCX_2$ group has begun to invert, allowing orbital overlap to develop, and (3) internal rotation about the CC bonds does not occur.

It has long been known that IRCs for dihalocarbene additions involve sequential bond formation,[6b,c,19] and Kraka and Cremer and co-workers have suggested the presence of intermediates in carbene additions based on their Unified Reaction Valley approach.[6g,h] However, these computational studies have not investigated the dynamical behavior of the intermediate. Experimentally, Zewail and co-workers have studied trimethylene and other diradicals directly. Using femtosecond-resolved photochemical generation of trimethylene from cyclobutanone in a molecular beam, Zewail measured a lifetime of 120 ± 20 fs for trimethylene.[20] Our trajectory-derived diradical lifetimes (below) are in that range.

**Involvement of $CX_2$ Inversion.** The involvement of $CX_2$ inversion during diradical cyclization is likely related to the well-known pyramidal structure of polyhalo-substituted radicals like

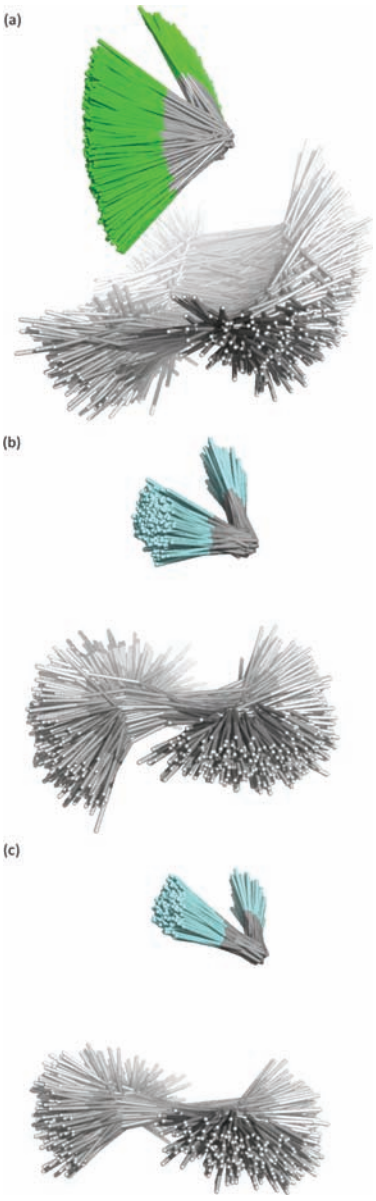


**Figure 2.** (a) Overlay of starting geometries of 453 reactive trajectories for the reaction of $CCl_2$ with ethylene. (b) Overlay of starting geometries of 466 reactive trajectories for $CF_2$ + ethylene on the UB3LYP/6-31G* surface. (c) Overlay of starting geometries of 298 reactive trajectories for $CF_2$ + ethylene on the mUB3LYP/6-31G* surface.

$CHX_2$. Ab initio potential energy barriers of inversion for $CHX_2$ radicals, corrected for zero-point vibrational energy (zpve), have been computed to be 0.5[21] and 6.3[22] kcal/mol for $CHCl_2$ and $CHF_2$, respectively. The zpve-corrected UB3LYP/6-31G* barriers of inversion have similar values of 0.5 and 5.8 kcal/mol for $CHCl_2$ and $CHF_2$, and for mUB3LYP/6-31G* the $CHF_2$ barrier is 5.7 kcal/mol. The inversion of $CF_2$ pyramidalization in the cyclization of hexafluorotrimethylene was studied computationally by Borden and co-workers.[23] The lowest energy transition state for cyclization involves simultaneous partial inversion of both $CF_2$ groups. With (6,6)CASPT2, the enthalpy of activation for this process is 9.8 kcal/mol at 150 °C.

The larger inversion barrier for a $CF_2$ diradical terminus relative to $CCl_2$ is expected to lengthen the diradical lifetime

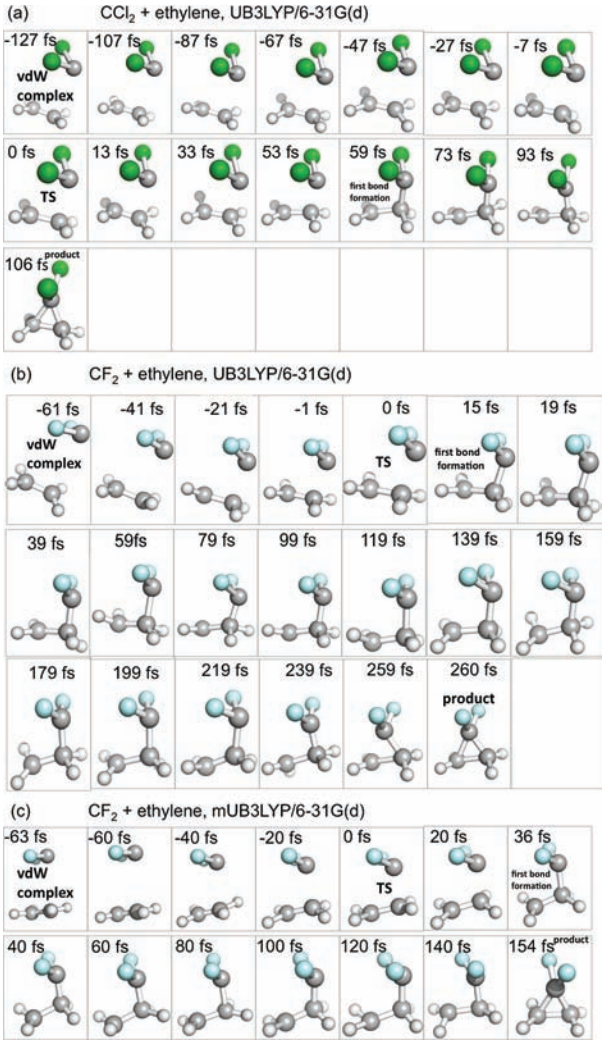


**Figure 3.** Snapshots of representative trajectories of the reaction of the carbene cycloadditions. Frames are snapshots starting from van der Waals complex via transition state and to product.

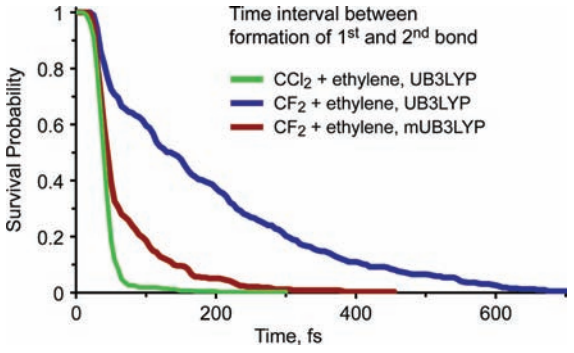


**Figure 4.** Lifetimes of diradicals formed in three sets of trajectories, computed as the time gap between formation of the first and second bonds (defined as C−C < 1.59 Å). Survival probability at time *t* is the fraction of diradicals that have not yet cyclized at time *t*. Time zero is the formation of the first bond.

by decreasing the probability of attaining the required partial inversion. Our measure for the diradical lifetime is the time gap

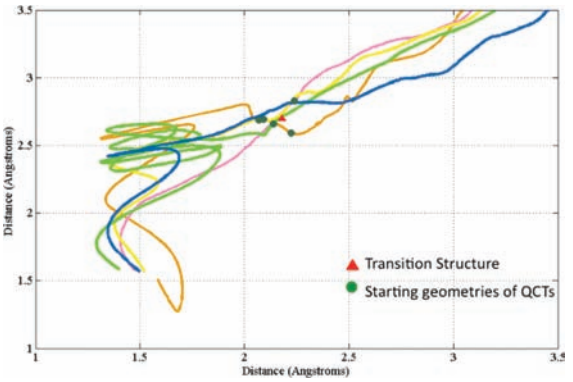


**Figure 5.** Five trajectories for $CCl_2$ + ethylene, projected onto the two forming C−C bond lengths.

between formation of the first and second bond, where bond formation is defined as a C−C distance less than 3 bohr, or 1.59 Å. That is, formation of the first bond defines the "birth" or appearance of the diradical, and formation of the second bond signifies its disappearance. Figure 4 shows the lifetimes computed in this way. With UB3LYP, Figure 4 shows a large difference in the lifetimes of the diradicals derived from $CCl_2$ and $CF_2$ additions to ethylene (green versus blue). However, the $CF_2$ diradical lifetimes computed with mUB3LYP are much shorter (red).

**UB3LYP and mUB3LYP Bracket the True Situation.** The reason for the difference between the UB3LYP and mUB3LYP description of $CF_2$ addition is likely complex. By design, there is no diradical minimum with mUB3LYP, and this must contribute to the difference. However, Figure 1b shows that the mUB3LYP flat region is severely truncated relative to UB3LYP and MRMP2-(10,10). One measure of this is the value of the CCC angle at the point along the IRC at which the energy starts to decrease rapidly. If we arbitrarily take this to be the point at which the gradient reaches −5 kcal/mol per bohr·amu$^{1/2}$, there is a clear difference among the methods shown in Figure 1b. For UB3LYP and MRMP2(10,10), this point is reached when CCC = 92°, but for mUB3LYP it is 97°. This gives the mUB3LYP diradical a narrower boundary within which to move while avoiding cyclization. Dynamics calculations of other diradicals have shown that trajectories with access to an extensive flat region may become trapped and behave like an intermediate.[24] On the other hand, a reduction in the size of the flat region is expected to shorten the lifetime of trajectories.

For these reasons, we suggest that the UB3LYP and mUB3LYP descriptions of $CF_2$ addition actually bracket the true situation. UB3LYP doubtless overestimates the lifetimes because it predicts a potential energy minimum, while mUB3LYP gives the diradical too small a range of motion within which to avoid cyclization. While a functional might be found in the future that better mimics MRMP2 or higher level results, we do not currently have the resources necessary for trajectories with MRMP2.

**Decay Patterns of Diradical Lifetimes.** The decay patterns in Figure 4 show a range of complexity. In the first 20−25 fs, there is no decay. This is the minimum time gap in the bond forming steps, the time needed, after formation of the first bond, for the diradical termini to move directly to within 1.59 Å. After 25 fs, each set of trajectories shows at least a fraction of very fast decay, followed by a variable amount of slower decay. The transition state for $CCl_2$ addition decays abruptly, with 95% decay in 65 fs after the first bond is formed. Decays of the $CF_2$ + ethylene

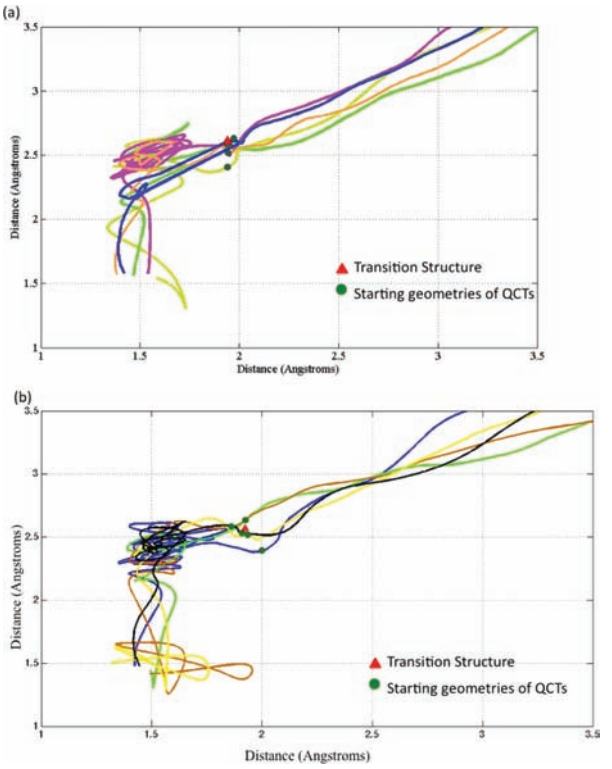


**Figure 6.** (a) Five trajectories for $CF_2$ + ethylene computed with UB3LYP/6-31G*, projected onto the two forming C−C bond lengths. (b) The same, computed with mUB3LYP/6-31G*.

diradicals in Figure 4 clearly have a long and short component. We fit these to biexponential decays; time constants of 15 and 190 fs were obtained for the UB3LYP calculations (amplitudes 0.55 and 0.45), and of 15 and 70 fs for mUB3LYP (amplitudes 0.15 and 0.85). This indicates a combination of direct cyclization and more complex motion, which is explored further below.

The ultrafast decay of the dichlorodiradical is consistent with the small barrier to $CCl_2$ inversion and indicates a dynamically direct reaction. This is not to say that the progress from diradical to cyclopropane is always uniform or monotonic. Figure 5 shows the two forming C−C bond lengths for five trajectories. Reactants are in the upper right corner, and product is located where the two bond lengths are about 1.5 Å. Trajectories were terminated when both bonds reached 1.59 Å. Four trajectories are very short-lived, with minimal oscillations. The fifth (green) is longer because the initial C−C bond retains its vibrational excitation for four oscillations before cyclizing. Once cyclized, about 15% of dichlorodiradical trajectories rebound back to CCC angles of 80−95° (C−C distances up to 2.4 Å), that is, back to the diradical region. This can persist for 2−3 large amplitude C−C excursions, which last up to 150 fs. However, no cyclopropane or diradical ever rebounded back to $CCl_2$ + ethylene. We saw no rebound from cyclopropane in the $CF_2$ case, possibly because F and C masses more nearly match so that vibrational redistribution out of C−C excitation is more efficient.[25]

Figure 6 shows five trajectories each for $CF_2$ + ethylene computed by UB3LYP and five computed by mUB3LYP. These span a range of lifetimes and include examples of trapped trajectories as well as more direct trajectories. The trajectories travel in a more-or-less horizontal rather than diagonal fashion that would be expected for synchronous bond formation, and

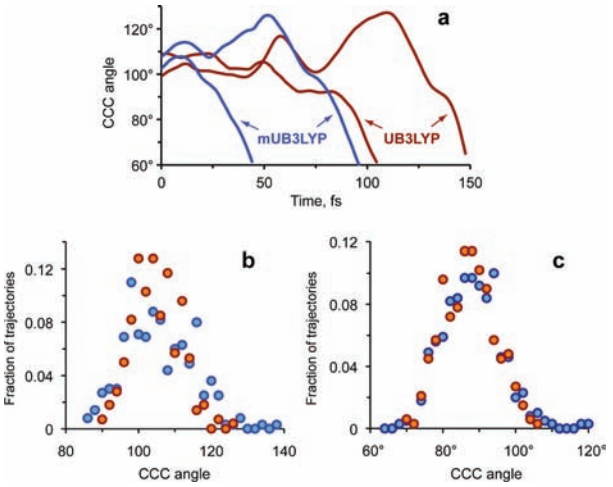


**Figure 7.** (a) Motion of CCC angle $\theta$ in trajectories for $CF_2$ + ethylene computed by UB3LYP and mUB3LYP. Two trajectories are shown for each method. (b) Distribution of the final $\theta$ turning point of each trajectory prior to cyclization. Red, mUB3LYP; blue, UB3LYP. (c) Distribution of the value of $\theta$ at the point at which $\varphi = 90°$ (planar). Colors as in (b).

inertial effects cause one bond to fully form and then to oscillate sometimes many times as energy is distributed in such a way that the $CF_2$ center can invert and the second bond can form.

The slower decay components of the difluorodiradicals are exemplified in Figure 3b, in which the $CF_2$ group maintains its original endo orientation for over 200 fs, preventing cyclization until inversion occurs. The CCC angle $\theta$ oscillates several times, but no cyclization occurs until the $CF_2$ inverts. This behavior contrasts with trimethylene,[24a] in which $CH_2$ inversion is nearly barrierless, and in which a decrease in $\theta$ in a face-to-face orientation like Figure 3b would lead to cyclization. It appears that the rate-determining step for cyclization is energy flow into $CF_2$ pyramidalization, which is coupled to the two C−C stretches and CCC bending. In the absence of an analysis of mode−mode energy transfer, we can achieve some insight by monitoring $\theta$ and the $CF_2$ pyramidalization angle $\varphi = (d_1 - d_2 + 360°)/2$, where the CCCF dihedral angles $d_1$ and $d_2$ obey $0° < d_1, d_2 < 360°$, and $d_1 < d_2$. With this definition, $\varphi < 90°$ implies endo paramidalization as in Figure 3, $\varphi = 90°$ is the planar geometry, and $\varphi > 90°$ is the exo paramidalization adopted only as cyclopropane is forming.

**Turning Points Analysis.** Figure 7a shows typical $\theta$ motion in a pair of trajectories each for UB3LYP and mUB3LYP. The number of turning points (extrema) varies from 1 for the shortest trajectory, to 5−7 for the longer trajectories, which can undergo large variations in $\theta$. Over the full set of UB3LYP and mUB3LYP trajectories, the number of $\theta$ turning points increases roughly in proportion to the lifetime, but throughout this motion $\varphi$ remains endopyramidalized until cyclization occurs. During this time, $\varphi$ also undergoes small oscillations, mainly between 60° and 75°. In 15% of trajectories, $\varphi$ rises to 80−87° during these oscillations. Figure 7b shows the distribution of the final $\theta$ turning point in each trajectory prior to cyclization. These are the values of $\theta$ at which cyclization begins to occur. At the final $\theta$ turning point, or at most 10 fs later, $\varphi$ starts to increase monotonically (toward inversion) simultaneously with the monotonic decrease in $\theta$ toward cyclopropane. Figure 7c gives the distribution of $\theta$ at the point during the final approach to cyclopropane at which $\varphi = 90°$, the point of planarity at the inverting $CF_2$ group. All trajectories

**Table 2. Comparison of Time Gap of Bond Formation and Average Asynchronicity among Carbene Cycloadditions, 1,3-Dipolar Cycloadditions, and Diels−Alder Cycloadditions**

| | time gap of bond formation (fs)[a] | average asyncronicity (Å)[a] |
|---|---|---|
| carbene cycloadditions | 50−250 | 0.54−0.67 |
| 1,3-dipolar cycloadditions | 10−30[b] | 0.18−0.30[b] |
| Diels−Alder cycloadditions | 5−60[c] | 0.15−0.83[c] |

[a] Average values. [b] Data adapted from our previous papers on 1,3-dipolar cycloadditions.[10] [c] Black, K.; Liu, P.; Xu, L.; Doubleday, C. E.; Houk, K. N., unpublished results.

that reach this point continue on to cyclopropane. In most cases, the point at which $\varphi = 90°$ occurs within 15−30 fs of the end. The mean values in Figure 7b and c are about 20° apart.

In about one-half of the trajectories longer than 100 fs, the final $\theta$ turning point (Figure 7b) is preceded ca. 20−50 fs earlier by an increase in $CF_2-CH_2$ bond length to 1.65−1.75 Å. The subsequent C−C compression occurs during or slightly before the final $\theta$ turning point and subsequent rush toward $CF_2$ inversion and cyclization. This sequence is consistent with energy transfer from C−C stretching to $CF_2$ inversion, which allows cyclization to occur.

**Direct and Complex Mechanisms.** The present study includes diradical lifetimes ranging from well under 100 fs to over 600 fs, with biexponential decay in the $CF_2$ case and approximately single exponential decay for $CCl_2$. These reactions are well-known to be stereospecific, and their classification as concerted seems uncontroversial. At femtosecond time resolution, however, an intermediate may be identified spectroscopically, whether or not it can be trapped or its stereochemistry affected. Carpenter[27] has pointed out that the concerted/stepwise classification encounters a problem if the definition of an intermediate is not clear. By studying the distribution of bond formation intervals and turning points of carbene additions, we have attempted to identify direct trajectories by their short lifetimes and uncomplicated progress toward product. In these reactions, direct product formation occurs within 60−70 fs after the first bond is formed. That includes essentially all dichlorodiradicals and about one-half of the difluorodiradicals. This is an appropriate time frame for direct motion in these reactions, because 60−70 fs is the time scale of CCC angle bending and C−C stretching, which are associated with the reaction coordinate for cyclization. For other reactions with lower characteristic frequencies for the modes that lead to reaction (internal rotation, for example), a longer time scale criterion for direct reactions is appropriate. For longer lived difluorodiradicals, the motion is complex, not direct, as CCC bending encounters an increasing number of inner turning points.

Experimentally, the reactions of $CF_2$ with *trans*-2-butene and *cis*-2-butene are stereospecific.[28] The dynamic simulations of the reaction of $CF_2$ with *trans*-2-butene and *cis*-2-butene are in progress.[29] For the trajectories obtained so far, we have observed that there is no rotation along the double bond during the cycloaddition, as is found in experiment. This is consistent with Firestone's cyclo-diradical mechanism that he proposed for 1,3-dipolar and Diels−Alder cycloadditions.[30] For those reactions, we find, by contrast, dynamically concerted mechanisms.[10]

As a measure of the degree of asymmetry in the distribution of forming pairs of bonds on the TS dividing surface, we define the average asynchronicity as the difference between the two forming bonds averaged over all sampled TS points. This is complementary to the bond formation time gap, which is dynamically based. For $CCl_2$ + ethylene, the average asynchronicity is 0.54 ± 0.13 Å (±standard deviation). For $CF_2$ + ethylene, the average asynchronicity is 0.67 ± 0.12 and 0.66 ± 0.11 Å for UB3LYP and mUB3LYP, respectively.[26]

**Comparison among Carbene, 1,3-Dipolar, and Diels−Alder Cycloadditions.** Table 2 shows the time gaps of bond formation and average asynchronicity among carbene cycloadditions, 1,3-dipolar cycloadditions, and Diels−Alder cycloadditions that we have studied. As expected, the largest time gaps in bond formation occur for carbene cycloadditions, which include a large contribution from complex dynamics in the difluorodiradicals. The largest asynchronicities, on the other hand, are observed in Diels−Alder reactions, larger even than carbene additions, which have asymmetric saddle points. (Large Diels−Alder asynchronicities are associated with highly asymmetric substitution. In symmetric cases, asynchronicities are 0.16−0.21 Å). The difference in Table 2 in the criteria for asymmetry highlights their complementary focus, one on the TS, the other on the subsequent dynamics. By both criteria, dipolar cycloadditions are among the clearest examples of concerted bimolecular reactions.

## CONCLUSIONS

In summary, the trajectory simulations provide for the first time a detailed dynamical picture of how carbenes react with alkenes, especially the timing of bond formation and a detailed description of dihalodiradical cyclization. A dynamical classification of reaction mechanism is discussed. The trajectories always have pronounced nonleast motion approach character. The reaction of $CCl_2$ with alkenes is a dynamically direct or concerted process with average time gap of bond formation of around 50 fs. The reaction of $CF_2$ with ethylene occurs with biexponential decays of short and long time constants. The short component is a direct or concerted process. The long component is dynamically complex, in the sense of a temporarily trapped diradical trajectory in a region with no potential energy minimum. This can also be called dynamically stepwise, where the second step refers to decay of an intermediate that could in principle be spectroscopically observed. Previous studies of 1,3-dipolar cycloaddition[10,31] and Diels−Alder reactions[32,33] show dynamically concerted behavior, with several examples of product selectivity based on post-TS dynamics. The stepwise 2 + 2 cycloaddition of cyclopentyne to ethylene has also been investigated, and the forbidden process has intermediate lifetimes sufficient for stereochemical scrambling.[34]

## ASSOCIATED CONTENT

**Supporting Information.** Complete ref 15, and optimized geometries and energetics of all of the stationary points for the reaction of $CCl_2$ and $CF_2$ with ethylene. This material is available free of charge via the Internet at http://pubs.acs.org.

## AUTHOR INFORMATION

**Corresponding Author**
houk@chem.ucla.edu; ced3@columbia.edu

## ACKNOWLEDGMENT

We are grateful to the National Science Foundation (CHE-0548209 to K.N.H. and CHE-0910876 to C.E.D.) for financial

support. Computer time was provided in part by the National Center for Supercomputing Applications (NCSA) on Abe (TG-CHE040013N to K.N.H. and TG-CHE090070 to C.E.D.), and by the UCLA Institute for Digital Research and Education (IDRE). We thank Prof. Robert A. Moss and Prof. Karsten Krogh-Jespersen for helpful comments.

## REFERENCES

(1) Hine, J. *J. Am. Chem. Soc.* **1950**, *72*, 2438–2445.
(2) Doering, W.; von, E.; Hoffmann, A. K. *J. Am. Chem. Soc.* **1954**, *76*, 6162–6165.
(3) Skell, P. S.; Garner, A. Y. *J. Am. Chem. Soc.* **1956**, *78*, 5430–5433.
(4) Moore, W. R.; Moser, W. R.; LaPrade, J. E. *J. Org. Chem.* **1963**, *28*, 2200.
(5) Hoffmann, R. *J. Am. Chem. Soc.* **1968**, *90*, 1475.
(6) (a) Zurawski, B.; Kutzelnigg, W. *J. Am. Chem. Soc.* **1978**, *100*, 2654–2659. (b) Rondan, N. G.; Houk, K. N.; Moss, R. A. *J. Am. Chem. Soc.* **1980**, *102*, 1770. (c) Houk, K. N.; Rondan, N. G.; Mareda, J. *J. Am. Chem. Soc.* **1984**, *106*, 4291–4293. (d) Blavins, J. J.; Cooper, D. L.; Karadakov, P. B. *Int. J. Quantum Chem.* **2004**, *98*, 465. (e) Merrer, D. C.; Rablen, P. R. *J. Org. Chem.* **2005**, *70*, 1630. (f) Lecea, B.; Ayerbe, M.; Arrieta, A.; Cosso, F. P.; Branchadell, V.; Ortuo, R. M.; Baceiredo, A. *J. Org. Chem.* **2007**, *72*, 357. (g) Joo, H.; Kraka, E.; Quapp, W.; Cremer, D. *Mol. Phys.* **2007**, *105*, 2697–2717. (h) Kraka, E.; Cremer, D. *Acc. Chem. Res.* **2010**, *43*, 591–601. (i) Gao, X.; Ohtsuka, Y.; Ishimura, K.; Nagase, S. *J. Phys. Chem. A* **2009**, *113*, 9852–9860.
(7) Keating, A. E.; Merrigan, S. R.; Singleton, D. A.; Houk, K. N. *J. Am. Chem. Soc.* **1999**, *121*, 3933–3938.
(8) (a) Chapman, S.; Bunker, D. L. *J. Chem. Phys.* **1975**, *62*, 2890. (b) Muckerman, J. T. *Theoretical Chemistry*; Academic Press: New York, 1981; Vol. 6, part A, Chapter 1. (c) Truhlar, D. G.; Duff, J. W.; Blais, N. C.; Tully, J. C.; Garrett, B. C. *J. Chem. Phys.* **1982**, *77*, 764. (d) Peslherbe, G. H.; Wang, H.; Hase, W. L. *J. Am. Chem. Soc.* **1996**, *118*, 2257. (e) Peslherbe, G. H.; Hase, W. L. *J. Chem. Phys.* **1996**, *104*, 7882. (f) Debbert, S. J.; Carpenter, B. K.; Hrovat, D. A.; Borden, W. T. *J. Am. Chem. Soc.* **2002**, *124*, 7896–7897. (g) Vayner, G.; Addepalli, S. V.; Song, K.; Hase, W. L. *J. Chem. Phys.* **2006**, *125*, 14317.
(9) Wang, I. S. Y.; Karplus, M. *J. Am. Chem. Soc.* **1973**, *95*, 8160–8164.
(10) (a) Xu, L.; Doubleday, C. E.; Houk, K. N. *Angew. Chem., Int. Ed.* **2009**, *48*, 2746–2748. (b) Xu, L.; Doubleday, C. E.; Houk, K. N. *J. Am. Chem. Soc.* **2010**, *132*, 3029–3037.
(11) Grimme, S.; Antony, J.; Ehrlich, S.; Krieg, H. *J. Chem. Phys.* **2010**, *132*, 154104.
(12) In Gaussian 09, mUB3LYP is specified by UBLYP with IOp(3/76=1000001200), IOp(3/77=0720008800), IOp(3/78=0810010000).
(13) Hase, W. L.; Duchovic, R. J.; Hu, X.; Komornicki, A.; Lim, K.; Lu, D.-H.; Peslherbe, G. H.; Swamy, K. N.; Vande Linde, S. R.; Wang, H.; Wolfe, R. J. *VENUS 96 QCPE* 1996; p 671.
(14) (a) Chapman, S.; Bunker, D. L. *J. Chem. Phys.* **1975**, *62*, 2890–2899. (b) Peslherbe, G. H.; Wang, H.; Hase, W. L. *Adv. Chem. Phys.* **1999**, *105*, 171–201. (c) Doubleday, C.; Bolton, K.; Hase, W. L. *J. Phys. Chem. A* **1998**, *102*, 3648–3658.
(15) Frisch, M. J.; et al. *Gaussian 09*, revision A.1; Gaussian, Inc.: Wallingford, CT, 2009. Full reference can be found in the Supporting Information.
(16) Truhlar, D. G.; Garrett, B. C.; Klippenstein, S. J. *J. Phys. Chem.* **1996**, *100*, 12771–12800.
(17) Houk, K. N.; Rondan, N. G. *J. Am. Chem. Soc.* **1984**, *106*, 4293–4294.
(18) We have previously used the arbitrary values of 1.6 and 2.0 Å. The latter is closer to the TS and gives a time gap of 52 fs for the trajectory.[9]
(19) Bernardi, F.; Bottoni, A.; Canepa, C.; Olivucci, M.; Robb, M. A.; Tonachini, G. *J. Org. Chem.* **1997**, *62*, 2018 and references therein.
(20) Pedersen, S.; Herek, J. L.; Zewail, A. H. *Science* **1994**, *266*, 1359. See also a dynamics simulation of the trimethylene diradical: Doubleday, C.; Bolton, K.; Peslherbe, G. H.; Hase, W. L. *J. Am. Chem. Soc.* **1996**, *118*, 9922–9931.
(21) Kafafi, S.; Hudgens, J. W. *J. Phys. Chem.* **1989**, *93*, 3474–3479.
(22) Fudacz, P. S.; Dober, J. D.; Jarman, D. L.; Standard, J. M.; Quandt, R. W. *J. Phys. Chem. A* **2003**, *107*, 9730–9735.
(23) Wei, H.; Hrovat, D. A.; Dolbier, W. R., Jr.; Smart, B. E.; Borden, W. T. *Angew. Chem., Int. Ed.* **2007**, *46*, 2666–2668.
(24) (a) Doubleday, C; Bolton, K; Peslherbe, G. H.; Hase, W. L. *J. Am. Chem. Soc.* **1996**, *118*, 9922–9931. (b) Doubleday, C. *J. Phys. Chem. A* **2001**, *105*, 6333–6341. (c) Doubleday, C.; Suhrada, C. P.; Houk, K. N. *J. Am. Chem. Soc.* **2006**, *128*, 90–94.
(25) For the $CCl_2$ reaction, there is a mixture of concerted direct pathways, with 95% of the trajectories leading to formation of both bonds in less than the lifetime (~60 fs) of a CC stretching vibration. Only 5% would be considered to explore the diradical surface for more than one vibrational lifetime.
(26) The average asynchronicities, measured by the difference in bond lengths in the transition state, are not so different for the $CCl_2$ and $CF_2$ reactions, but the lifetimes of the diradicals formed after the first bond formation are very different.
(27) (a) Carpenter, B. K. *Angew. Chem., Int. Ed.* **1998**, *37*, 3340–3350. (b) Carpenter, B. K. *Acc. Chem. Res.* **1992**, *25*, 520–528.
(28) Mitsch, R. A. *J. Am. Chem. Soc.* **1965**, *87*, 758–761.
(29) Xu, L.; Doubleday, C. E.; Houk, K. N., unpublished results.
(30) Firestone, R. A. *J. Org. Chem.* **1968**, *33*, 2285–2290.
(31) Vayner, G.; Addepalli, S. V.; Song, K.; Hase, W. L. *J. Chem. Phys.* **2006**, *125*, 014317.
(32) (a) Huang, C.; Tasi, L.; Hu, W. *J. Phys. Chem. A* **2001**, *105*, 9945–9953. (b) Aktah, D.; Passerone, D.; Parrinello, M. *J. Phys. Chem. A* **2004**, *108*, 848–854. (c) Kelly, E.; Seth, M.; Ziegler, T. *J. Phys. Chem. A* **2004**, *108*, 2167–2180. (d) Nao Noguchi, N.; Nakano, H. *J. Chem. Phys.* **2009**, *130*, 154309-1–11.(e) Black, K.; Liu, P.; Xu, L.; Doubleday, C. E.; Houk, K. N., unpublished results.
(33) (a) Thomas, J. B.; Waas, J. R.; Harmata, M.; Singleton, D. A. *J. Am. Chem. Soc.* **2008**, *130*, 14544–14555. (b) Wang, Z. H.; Hirschi, J. S.; Singleton, D. A. *Angew. Chem., Int. Ed.* **2009**, *48*, 9156–9159.
(34) Glowacki, D. R.; Marsden, S. P.; Pilling, M. J. *J. Am. Chem. Soc.* **2009**, *131*, 13896–13897.